Department of
Physics

Queen's University
Kingston, Canada

DEVELOPMENT OF ELECTRODES FOR SOLID ELECTROLYTES

FINAL REPORT - PHASE II

February 1986

M.F.BELL AND M.SAYER

Department of Physics

Queen's University at Kingston

Department of Supply and Services

Contract # OST84-00347

DSS File # 21ST.23440-4-9204

MICROMEDIA

JUL 10 1986

43pp

CONTENTS

	Page
Executive Summary	i.
Resume administratif	ii.
Personnel	iii
1. Introduction	1
2. Material Selection	2
2.1 Electrochemical aspects	3
2.2 Physical aspects	5
- Electrical Conductivity	5
- Porosity	5
2.3 Conclusions	6
2.4 Proton conducting substrates	7
3. Electrode Preparation	9
3.1 Chemical deposition	9
- platinum	10
- $NiCo_2O_4$	12
- RuO_2	12
3.2 Physical Deposition	13
- Reactive sputtering of La_2NiO_4	13
- Plasma spraying of molybdenum	13
4. Characterisation Procedures	16
4.1 Electrical resistivity	16
4.2 Porosity	18

5. Material Characterisation 24

5.1 Molybdenum 24

5.2 Nickel cobalt oxide 26

5.3 Ruthenium dioxide 31

6. Steam Cell Design and Lifetime Measurements 33

6.1 Electrode lifetime 35

- platinum 35

- molybdenum/$NiCo_2O_4$ 35

7. Summary and Conclusions 37

Acknowledgements 38

References 39

EXECUTIVE SUMMARY

Electrode materials have been investigated for use in hydrogen-oxygen fuel cells based on proton conducting solid electrolytes such as H_3O^+-β/β''-aluminas. These include plasma-sprayed molybdenum, nickel cobalt oxide $NiCo_2O_4$, and ruthenium oxide RuO_2, with platinum being used as a standard of comparison. Molybdenum is recommended for use as the hydrogen electrode, while $NiCo_2O_4$ shows considerable promise as an oxygen electrode.

Methods are developed for film fabrication, characterisation and use in specially designed steam cells. The evaluation methods include four-probe conductivity measurements, and a technique for evaluation of film porosity.

All three materials are stable in steam at 300°C, but platinum degrades in acidic environments and/or under strong hydrogen flow within the electrolyte.

RESUME ADMINISTRATIF

Les électrolytes solides ont été testés pour être utilisés dans des cellules à combustible hydrogène - oxygène ; l'exemple type est l'alumine β/β" conductrice ionique du proton H_3O^+. Nous citerons comme materiaux électrolytiques : le molybdène obtenu par projection au plasma, l'oxyde spinelle de nickel et cobalt $NiCo_2O_4$, et l'oxyde de ruthénium, RuO_2, avec le platine utilisé comme référence. Le molybdène est recommandé pour être utilisé en tant qu'électrode à hydrogène et $NiCo_2O_4$ paraît très prometteur pour une application en tant qu'électrode à oxygène.

La fabrication des films, leur characterisation et utilisation dans des cellules à vapeur spécialement conçues sont actuellement à l'étude. Des mesures de conductivité à quatre points ainsi qu'une technique d'évaluation de la porosité des films sont menées en parallèle.

Tous ces materiaux sont chimiquement stables dans la vapeur à 300°C. Toutefois le platine se dégrade en environnement acide et/ou sous un flux très fort d'hydrogène au sein de l'electrolyte.

PERSONNEL

Queen's University

M.F.Bell	Principal Investigator
M.Sayer	Principal Investigator
B.A.Judd	Research Scientist
Y.Koskinen	Summer Student
T.M.Hood	Summer Student

Sub-contract: McMaster University

P.S.Nicholson	Principal Investigator

1. INTRODUCTION

Solid electrolytes are polycrystalline materials in which the movement of ions results in high conductivity. This combined with negligible electronic conductivity allows their use in a number of devices including gas sensors, ion sensors, secondary batteries, water electrolysis units and fuel cells. Although a number of technologically interesting materials have been developed over the past decade, their application has been hindered by a lack of knowledge of suitable electrode materials. One example is the use of a hydrogen ion conductor, e.g. hydronium β" alumina, in a hydrogen-air fuel cell where platinum has been employed because of its high catalytic ability. However the metal is prohibitively expensive and our attention has been focussed on developing alternative materials.

The selection of these materials was based on a theoretical simulation which relied heavily on performance data obtained in liquid electrolyte cells. This was carried out in the first year of this contract and will be only briefly summarised in the second section of this report[1].

The major thrust of this phase has been to prepare the selected materials on a number of substrates and to carry out preliminary measurements to determine their physical and chemical characteristics. These experiments are described in sections 3 and 4.

The concluding section will attempt to choose the optimum electrode system and discuss the future experimental work necessary to confirm these predictions.

2. MATERIAL SELECTION

The selection of suitable electrode materials depends strongly on the device design. As shown schematically in Fig. 2.1, the device consists of two porous electrodes supported by a solid electrolyte.

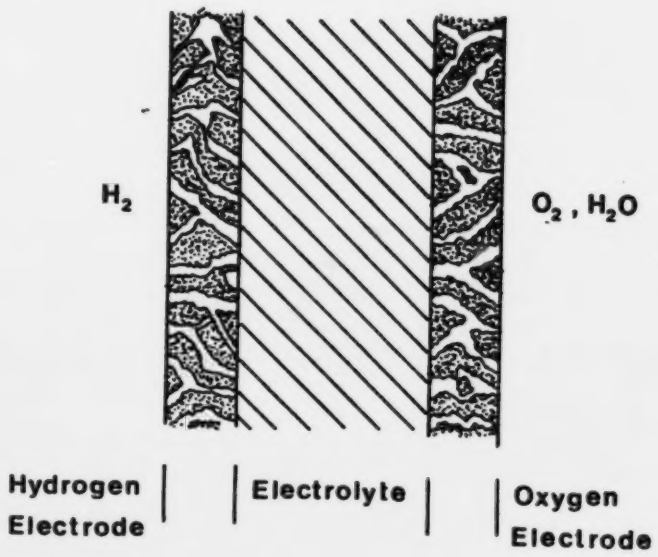

Figure 2.1: Electrochemical cell using a solid electrolyte.

The gaseous reactants must pass through the electrodes by gaseous diffusion to the electrode/electrolyte interface where they will react to produce a current. Thus it can be seen that the choice of material will depend not only on the electrochemistry of the interface but also on the physical characteristics of the electrode structure.

This includes both its porosity to gaseous diffusion and electrical resistance. These aspects will be discussed in this section.

2.1 Electrochemical Aspects

In describing the behaviour of an electrode/electrolyte interface, it is usual to describe the potential barrier for charge transfer in terms of the Bultler-Volmer equation (eqn. 2.1) which relates the current density, i, to the activation overpotential, η,:

$$i = i_o \left\{ \exp - \frac{\alpha n F \eta}{RT} + \exp \frac{(1-\alpha) m F \eta}{RT} \right\} \quad (2.1)$$

where α is the transfer coefficient and i_o is the exchange current density. In the case of solid electrolytes, it has been shown that a Frumkin type correction should be applied to account for the presence of only one mobile ion and thus the absence of a diffuse double layer. However, this correction is expected to be small and equation 2.1 will be adequate in predicting the interfacial behaviour. The exchange current density is of fundamental importance in that it is related to the height of the activation barrier by an equation of the form:

$$i_o = A \exp(G^*/RT)$$

where G^* is the activation energy and, for the hydrogen reaction is typically of the order of 75 $kJ.mol^{-1}$. This allows us to predict that to achieve adequate operating levels at the proposed operating temperature of 300°C, the material for the hydrogen electrode should have an i_o

between 10^{-6} and 10^{-7} A.cm^{-2} at room temperature. Comparison of the data given in Table 2.1 shows that this restricts our choice to transition metals and the most sensible choices seem to be nickel and molybdenum. Partly because of its ease of preparation by the commercially viable plasma spray technique, molybdenum was chosen for further investigation.

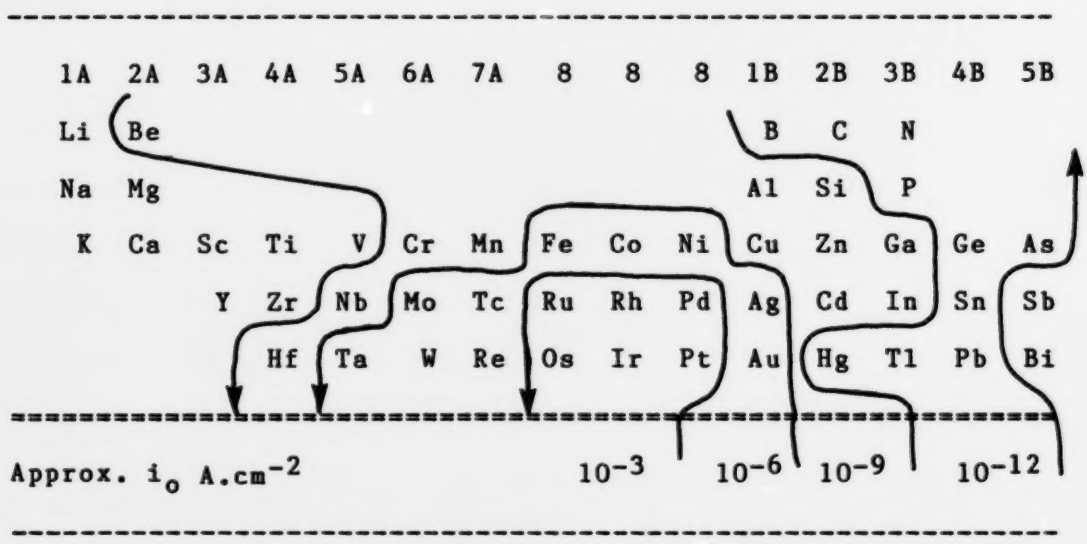
1A 2A 3A 4A 5A 6A 7A 8 8 8 1B 2B 3B 4B 5B
Li Be B C N
Na Mg Al Si P
K Ca Sc Ti V Cr Mn Fe Co Ni Cu Zn Ga Ge As
Y Zr Nb Mo Tc Ru Rh Pd Ag Cd In Sn Sb
Hf Ta W Re Os Ir Pt Au Hg Tl Pb Bi
Approx. i$_o$ A.cm^{-2}
10^{-3}
10^{-6}
10^{-9}
10^{-12}

Table 2.1: Hydrogen exchange current densities related to the periodic table

Data for the electrochemical behaviour of the oxygen electrode is less well established and relies more heavily on physical attributes of the materials themselves rather than the interfacial properties. It should be noted, however, that the two materials chosen, nickel cobalt oxide

and ruthenium dioxide, have shown high catalytic activity in cells operating close to room temperature.

2.2 Physical Aspects

The physical structure of an electrode plays an important role in determining the performance of a cell and, in particular, the electrical conductivity and porosity will play a major role.

2.2.1 Electrical Conductivity

As noted previously, the choice for the hydrogen electrode is molybdenum which, because of its metallic nature, is expected to have low resistivity and thus contribute negligible ohmic losses in cell performance. However it should be noted that, in the thin film form necessary to reduce the effects of gaseous diffusion, it will have a resistance higher than that of the bulk form and care must therefore be taken in preparation to achieve resistance values close to the bulk value. In contrast, the oxygen electrode will probably be a complex oxide which will exhibit semi-conducting properties. Thus it is necessary to choose materials exhibiting low resistivity such as $NiCo_2O_4$.

2.2.2 Porosity

Porosity plays an important role in cell performance in that low porosity will impede the flow of gas to the interface and thus cause a reduction in performance. In contrast, high porosity will, because of percolation

effects, increase the electrical resistance of the system. For this reason, we have chosen preparation techniques which we expect to result in optimum porosity. This is particularly important in the case of the semi-conducting oxides where the bulk resistivities are low. For this reason, we have decided to concentrate on reactive sputtering to produce thin films of lanthanum nickelate, La_2NiO_4, and chemical deposition to prepare electrodes of $NiCo_2O_4$ and RuO_2.

2.3 Conclusions

Consideration of the physical and electrochemical aspects of the electrode and its interface with the electrolyte has allowed us to choose four materials for further study. As has been shown, molybdenum is expected to have adequate catalytic activity at 300°C to operate as an efficient hydrogen electrode and moreover can be prepared by a commercially-viable plasma-spray technique. In contrast, three materials have been chosen to act as oxygen electrodes based on their known catalytic activity and the preparation techniques involved. These are La_2NiO_4, $NiCo_2O_4$ and RuO_2. As will be shown later, work carried out in the current year has allowed us to reduce this list to two promising candidates and one alternative.

2.4 Proton conducting substrates

This work was carried out on proton conducting electrolytes based on hydronium β/β'' aluminas. These materials have been developed in collaboration with Dr. P.S.Nicholson of McMaster University [2] and were obtained from this source. The fabrication process involves the preparation of a Na/K β/β'' alumina followed by a field assisted ion exchange to the proton analog. On completion of the exchange process, the sample contains mobile protons or H_3O^+ in the β'' phase, with immobile K^+ ions in the β-phase. The conductivity is shown as a function of temperature in Fig. 2.3 The conductivity is of the order of 10^{-4}-10^{-5} $ohms^{-1}cm^{-1}$ at 300K, but depends on the water content of the material. Thermogravimetric measurements show that water loss occurs reversibly above 200°C and irreversibly above 350°C. This is a significant factor for the preparation of electrodes. Electrode preparation on fully hydronium exchanged samples must be carried out below 300°C in order to retain the water content, while attempts to prepare electrodes by vacuum methods such as sputtering lead to poorly adherent layers through interaction of the sputtered metal ions with water vapour leaving the sample. An alternative is to fabricate electrodes on the precursor ceramic, prior to hydronium ion exchange. In this case, the electrode materials must be stable under the ion exchange and sufficiently porous for both liquids and gas to reach the interface with the electrolyte.

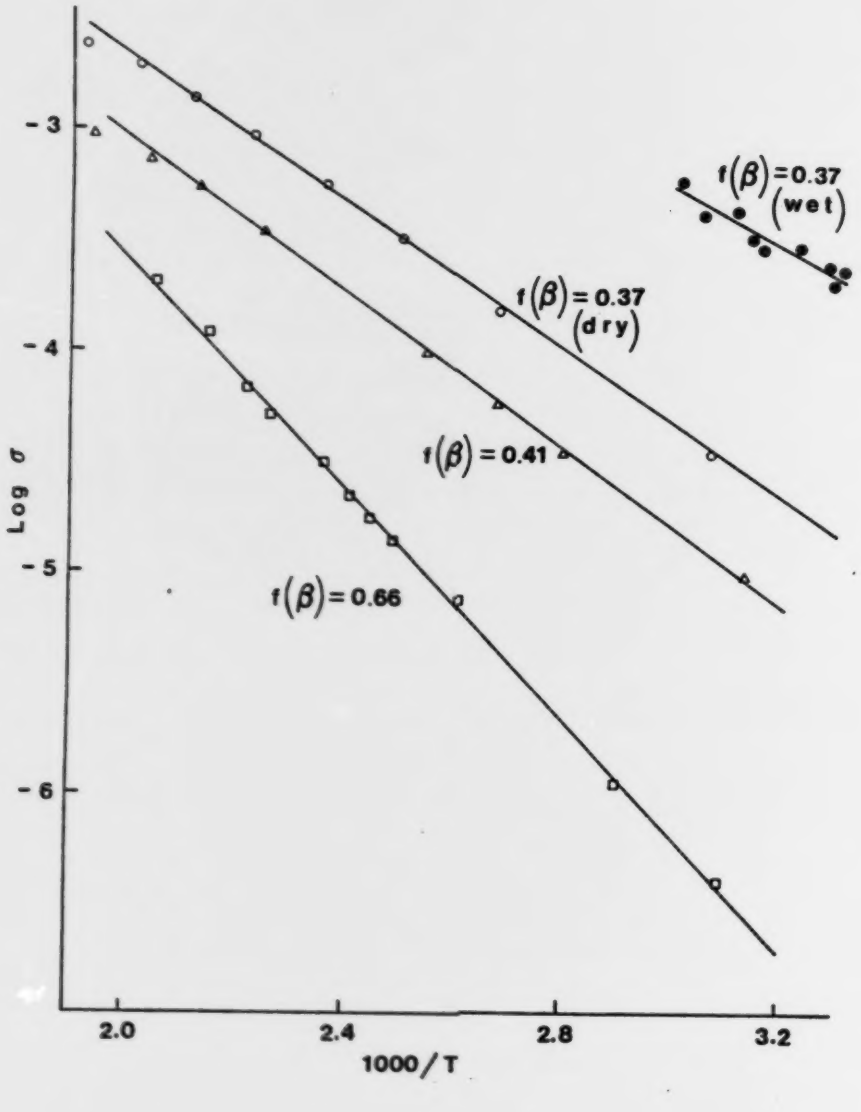

Figure 2.3: Proton conductivity versus temperature for polycrystalline H_3O β/β'' alumina ceramics

3. ELECTRODE PREPARATION

The ideal preparation technique would involve an ambient temperature and pressure route in which sample dehydration would not be a problem. Unfortunately the materials selected can only be prepared by use of high temperature or high vacuum techniques which results in some dehydration of the proton conductor. Our efforts in this year have been to modify these techniques to reduce dehydration to a minimum, However, it was found immediately that the exact procedure was specific to each electrode material although the preparation techniques can be broadly classified as chemical and physical deposition methods.

3.1 Chemical Deposition

Chemical deposition probably represents the most promising, commercially-viable preparation technique and can be summarised as dissolution of the electrode material or its precursor in a suitable solvent, followed by 'painting' of this solution on the electrolyte surface. The whole system is then subjected to a thermal treatment which removes the solvent and may involve decomposition of the precursor. In general, multiple coats are required to build up the required electrode thickness. Procedures for the fabrication of the electrode systems of interest are discussed in the following sections.

3.1.1 Platinum

The 'standard' electrode material for fuel cell applications is platinum. This is difficult to prepare in thin film form using physical methods, and therefore chemical deposition routes have been explored. These have included the use of commercially available pastes and paints in which platinum particles are dispersed in organic solvents. Platinum paste obtained from DeBussi initially showed good adhesion to such substrates as glass and zirconia but only poor adhesion to β alumina ceramics even with heat treatments as high as 850°C. This effectively eliminated this material and our attention was turned to platinum based paints in which smaller platinum particles were dispersed in a more volatile organic solvent. Englehard liquid bright platinum has been employed for this purpose. Although the manufacturer recommends a high temperature heat treatment, it was found that even a low temperature anneal ($\sim$300°C) resulted in films showing excellent adhesion to β -alumina ceramics. This was ascribed to the smaller particle size. The electrical resistance showed a strong dependence on the initial film thickness (Fig. 3.1) [3]. Thin films exhibited high electrical resistance because of the low metallic content. In contrast it proved difficult to remove all of the organic binder from thick films resulting again in high electrical resistance. This was solved in part by employing two novel approaches.

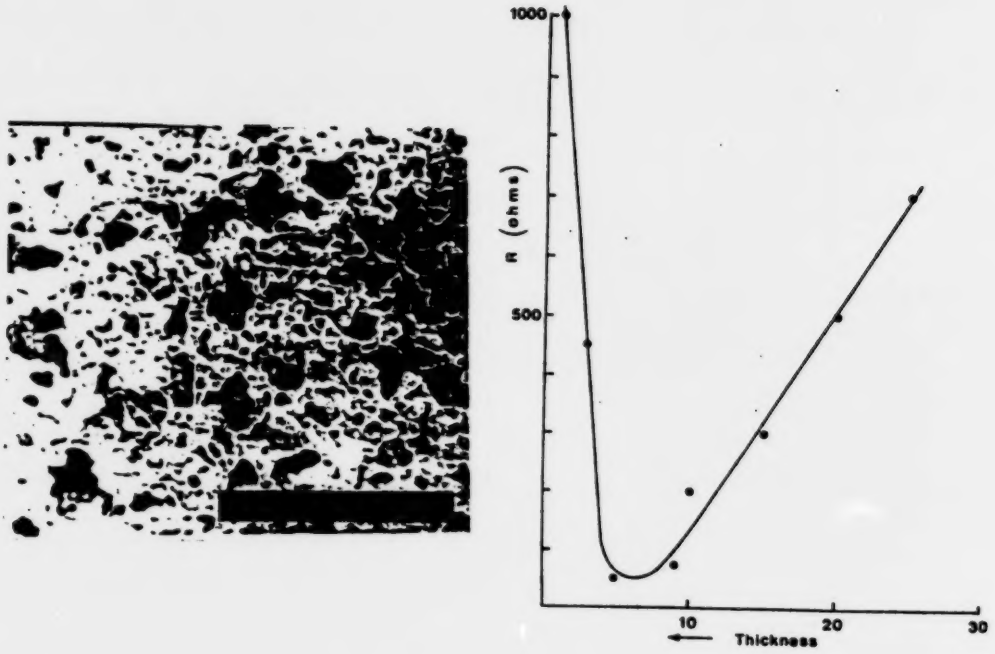

Figure 3.1 a) Resistance of fired platinum films as a function of film thickness.

b) Micrograph showing porous film structure of Pt electrodes.

This first involved the successive application of very thin coats which assisted the removal of the organics. Secondly the coats were baked under hydrogen to further reduce the organic binders to more volatile species. The micrograph in Fig.3.1 illustrates the excellent porosity achieved after such a procedure. Unfortunately the large number of parameters involved, e.g. the hydrogen pressure, curing temperature, etc., make it difficult to produce good electrodes on a reproducible basis. This problem can be compounded by unanticipated variations in the paint composition. After continuous success with an initial stock

of liquid bright platinum, the results became a dismal failure when the bottle was replaced. A third bottle then was successful again. However, if such effects can be avoided, hydrogen baked, liquid bright platinum electrodes fired at 300°C provide excellent electrodes for the purpose of a standard to which to compare alternatives.

An important observation for Pt electrodes on hydronium β/β'' alumina has been that the electrode is unstable in acid. This showed up particularly if ion exchange in dilute H_2SO_4 was carried out. The electrode flaked and then separated from the substrate.

3.1.2. Nickel Cobalt Oxide $NiCo_2O_4$

In the field of water electrolysis, $NiCo_2O_4$ has been prepared on nickel substrates by a number of techniques [4,5], the most interesting of which seems to be the decomposition of an aqueous solution of the respective nitrates. The process involves dissolution of nickel and cobalt nitrates in water followed by evaporation to produce a dark purple, super-saturated solution. When this is applied to the electrolyte surface and cured at 350°C, a strongly adherent, black film is produced.

3.1.3 Ruthenium Dioxide RuO_2

This material can again be prepared by thermal decomposition of aqueous solutions in a similar manner to $NiCo_2O_4$. In this case, the starting point is ruthenium chloro-hydrate, $RuCl_4.xH_2O$. The film was generally built by

successive coats of solution with each coat being fired at 300-400°C for 30-45 mins.

3.2 Physical Deposition

The most promising physical methods for the preparation of thin film electrodes are reactive sputtering and plasma (flame) spraying.

3.2.1 Reactive Sputtering of La_2NiO_4

Reactive sputtering has been used to produce thin films (<10 μm) of such materials as $Pb(Zr,Ti)O_3$ and ZrO_2 and involves the sputtering of metals in a reactive O_2 atmosphere [6]. Although the plasma chemistry is relatively complex, the films produced have excellent properties.

Our attempts to produce lanthanum nickelate by this technique have focussed on producing thin films on substrates such as glass and silicon. Preliminary results, however, suggested that the process resulted in lanthanum-rich phases deleterious to cell performance. Research on this material was therefore discontinued.

3.2.2 Plasma Spraying of Molybdenum

Plasma or flame spraying involves partially or wholly melting the material in an electric arc or oxy-acetylene torch before spraying it on to the cold substrate surface. It has been used widely in industry to produce surface coatings on automotive parts, etc. and

therefore seems commercially viable. In a separate contract to investigate a thermo-electric generator based on sodium ion conductors, molybdenum has been shown to be a promising electrode material and films have been produced on a number of substrates using this technique. The films produced have an average thickness of 20-30 μm and preliminary SEM pictures (Fig. 3.2) show them to have an open structure suggesting high porosity. On β alumina, however, care must be taken to remove any water from the substrate. Failure to do this causes formation of an interfacial layer of a hydrogen molybdenum bronze, H_xMoO_y, which results in poor adherency.

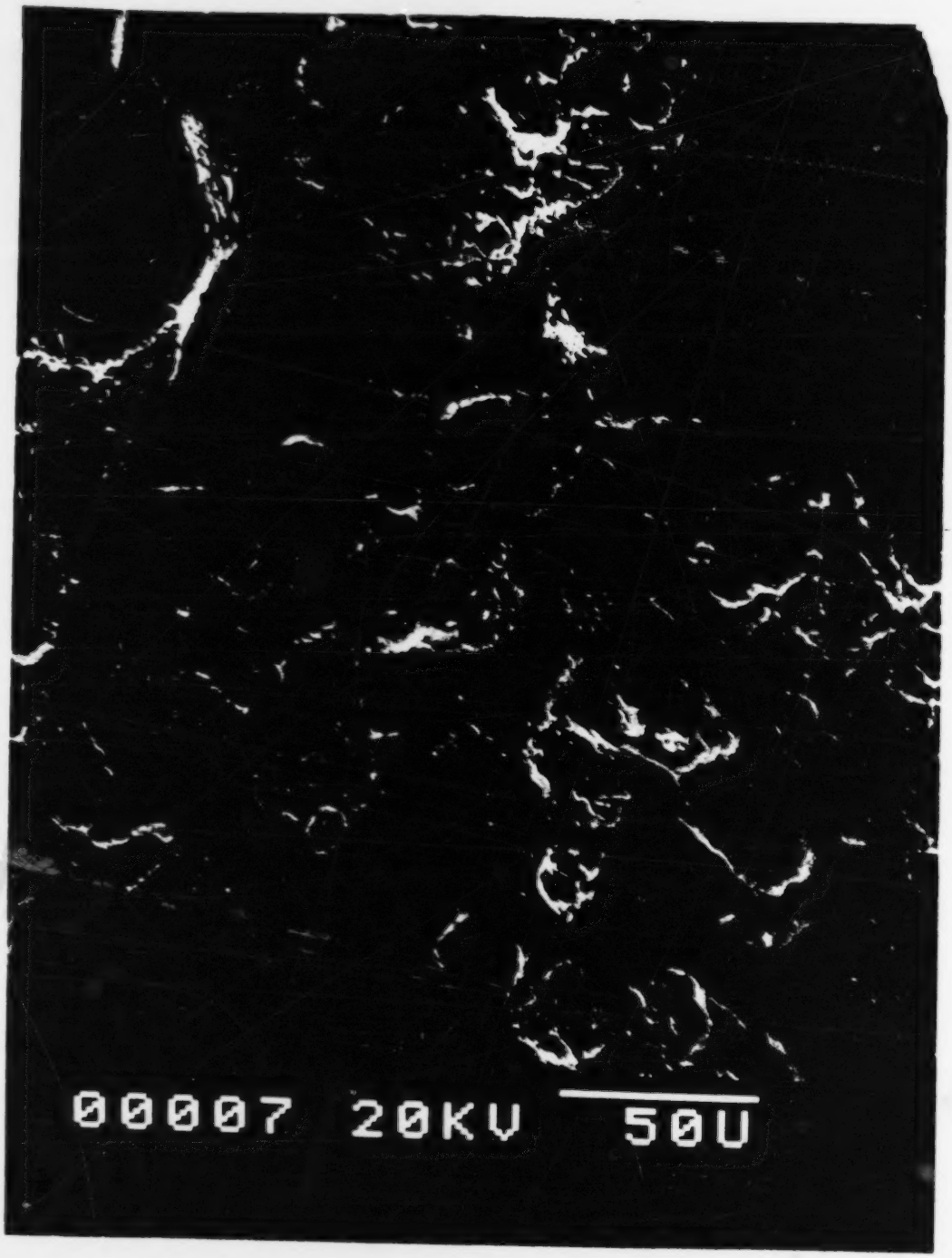

Figure 3.2: Micrograph of molybdenum thermally sprayed onto a Na β"-alumina substrate.

4. CHARACTERISATION PROCEDURES

Before the catalytic activity of an electrode can be successfully determined, it is necessary to measure the physical characteristics of the material itself. Two of the most important parameters are the electrical resistivity and porosity and the experimental procedures used to measure these will be described in this section.

4.1 Electrical Resistivity

The measurement of a thin, porous film is difficult for a number of reasons:

a) the geometry of the film does not lend itself to conventional two and four electrode techniques.

b) a thin film will not have the same resistivity as the bulk material.

c) Percolation effects will result in the electrical resistivity depending strongly on the porosity and therefore on the preparation technique.

Moreover, to compare the measurements to bulk values, it is necessary to obtain information on the temperature dependence of resistivity. For these reasons, we have employed a four probe method known as the van der Pauw technique which has

been shown to be applicable to thin slabs of material of arbitrary shape [7]. In this technique, the resistivity is measured by preparing four small contacts at arbitrary points on the circumference of a slab of material of thickness t (Fig. 4.1).

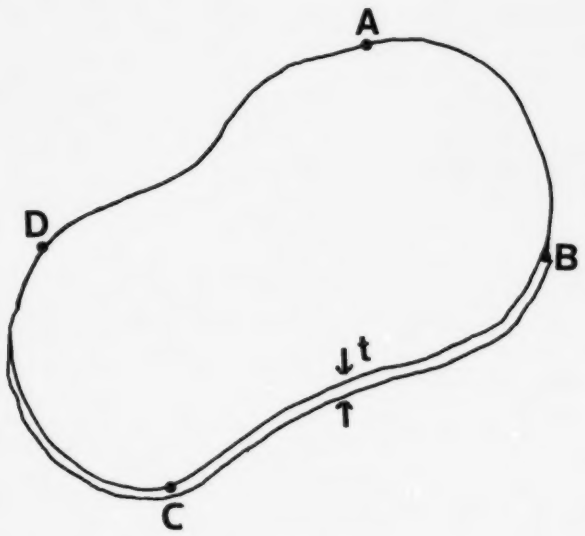

Figure 4.1: Sample configuration for a van der Pauw measurement

If a current, I_{AB}, flows through the contacts, AB, a voltage, V_{CD}, will be generated between C and D. Thus a resistance, $R_{AB,CD}$, can be defined as

$$R_{AB,CD} = V_{CD} / I_{AB}$$

Similarly $R_{BC,DA}$ can be defined as

$$R_{BC,DA} = V_{BC} / I_{DA}$$

From these resistances, the resistivity, ρ, can be calculated using the relation [7],

$$\exp\left\{-\frac{\pi R_{AB,CD} t}{\rho}\right\} + \exp\left\{-\frac{\pi R_{BC,DA} t}{\rho}\right\} = 1$$

where t is the film thickness. This equation is easily programmed on a personal computer.

4.2 Porosity

Gas flow through a porous medium is a complicated process involving diffusion, viscous flow and Knudsen flow [8]. At the high pressures expected in the present design, however, the gas flux, J, can be related to the gas pressure by an equation of the form [9]

$$J = -\frac{K}{kT}\left(\frac{\partial P}{\partial z}\right)$$

where K is termed the permeability coefficient which will depend on the geometry and k is Boltzmann's constant. For viscous flow, we can write from Poiseuilles Law,

$$J_{visc} = - \frac{n B_o}{\mu} \left(\frac{\partial P}{\partial z} \right)$$

where B_o is a viscous flow constant characteristic of the porous medium, μ is the viscosity of the gas, and n is the number density of the diffusing gas.

By substitution

$$K_v = (nkT) \frac{B_o}{\mu} = P_o \frac{B_o}{\mu}$$

where B_o is a constant characteristic of the porous medium. In the case of a single circular pore of radius r_o, B_o can be related to pore radius by $B_o = r_o^2/8$. This allows the definition of an effective pore size [8].

Similarly, for Knudsen flow, we can write

$$J_K = - D_K \left(\frac{\partial P}{\partial z} \right)$$

and therefore $K_T = D_K$ where D_K is the Knudsen diffusion coefficient and is dependent on both the gas and the material. However the Knudsen flow parameter K_o equals $3D_K/4v$, where v is the velocity of the molecule and K_o is solely dependent on the material [10].

As these flows are additive, the permeability coefficient, K_T, in the continuum regime will be

$$K_T = D_K + \frac{P_o B_o}{\mu}$$

Thus, to obtain information about the porosity, it is necessary to determine K at different pressure differentials and thus obtain values for B_o and D_K. If the flux J is defined as

$$J = \frac{n}{A} \left(\frac{\Delta V}{\Delta t} \right)$$

Then combining the equations above, we obtain

$$K = \frac{P_o}{\Delta P} \frac{L}{A} \frac{\Delta V}{\Delta t} \qquad (4.3)$$

where ΔP is the pressure differential at mean pressure P_o and L and A are the thickness and area of the diffusion membrane. The quantities in this equation are readily measured in the pressure regime above atmospheric using equipment such as that shown in figure 4.2. This is known as a 'Graham's Law' measurement in physical chemistry [10].

The apparatus consists of a glass vessel which can be filled with various gases through an inlet tube. The outlet tube is a Fischer filter tube consisting of a glass frit with a nominal pore size of 5 μm connected to a mercury reservoir by flexible tubing. By altering the height of this reservoir, the gas flow through the frit can be measured at pressures above atmospheric. Using the following procedures, the porosity of the material can be estimated:

1) The apparatus is evacuated and filled with an inert gas such as nitrogen or argon.
2) The reservoir is raised to increase the gas pressure by an amount, ΔP.
3) The time, Δt, for the gas to return to atmospheric by flowing through the frit is measured by electronically timing the flow of mercury in the flexible tubing. Δt is typically of the order of a few seconds.

4) Knowing the volume ΔV through which the mercury travels in time Δt, the constants B_o and D_K were calculated using the approximate formulae

$$K = \frac{P_o}{\Delta P} \frac{L}{A} \frac{\Delta V}{\Delta t} = D_K + P_o \frac{B_o}{\mu}$$

from which the pore radius r_o and $K_o = 3D_K/4v$ were estimated.

The above procedures were repeated for a number of pressures to test that the apparatus was operating in the continuum regime and with argon and hydrogen to verify that the flow rate was inversely proportional to the square root of the molecular weight of the gas [10]. The material to be tested was then deposited on the outer surface of the frit by the techniques described in section 3. The above procedures were repeated to determine the change in pore size. In all cases, the flow when the material was applied was substantially different from that for an uncoated frit, and the results were therefore characteristic of the coating.

The general parameters employed for the calculations were as follows:

Frit area:	6.95 cm^2
Frit thickness:	0.267 cm
Layer thickness:	$\sim 25\ \mu m$
Volume flow:	2.0 cm^3
Pressure difference:	0-0.26 atm
Viscosity (hydrogen):	8.59×10^{-7} N/cm-s
Viscosity (argon) :	2.17×10^{-6} N/cm-s

The major uncertainties in this experiment arise from the large scatter in the data tken over a restricted range of pressures and in estimating the effective thickness of the membrane. The mean pore size is also a crude approximation for the kind of path which must exist in the microstructure shown in fig.3.2. The glass frit filter constituted an easily available and economic substrate. In the case of RuO_2 and $NiCo_2O_4$, visual examination indicated that the material permeated the entire frit and therefore L could be estimated as the frit thickness. Plasma sprayed Mo was concentrated on the surface and L was estimated to be a smaller value. The mean slopes and intercepts calculated were evaluated knowing that particular relationships must exist between runs for different gases. The experimental data is shown in the discussion of each type of material.

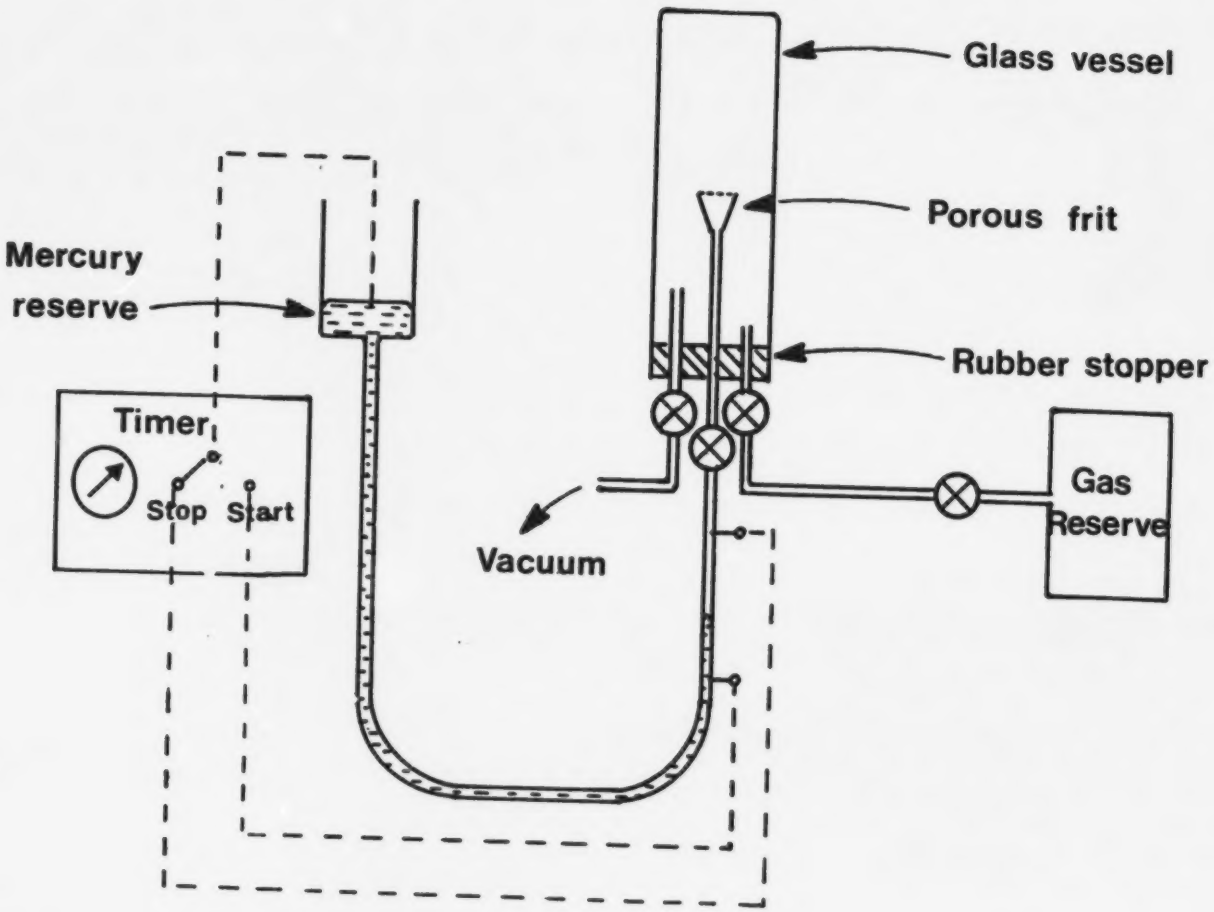

EXPERIMENTAL SETUP: POROSITY MEASUREMENT

5. MATERIAL CHARACTERISATION

5.1 Molybdenum

As shown in section 3., electron micrographs of molybdenum films produced by plasma spraying show a porous structure which is qualitatively confirmed by porosity measurements using glass frits (section 4.2). Values of K measured using helium and argon respectively are shown in Fig. 5.1. The data show a large amount of scatter caused by pressure oscillations during the course of the experiment. Calculations of the pore size from B_o and D_K give a value of $r_o = 4.5 \pm 1.0\,\mu m$ for the pore radius which should result in a high porosity in these 20-30 μm films. The accuracy of the measurements was limited by the small pressure range of the measurements and the large scatter in the measured data.

The sheet resistance at room temperature was 20 mohms/sq, which is only 10 times that of bulk molybdenum. Moreover the resistivity increased linearly with temperature indicating metallic behaviour. The temperature coefficient estimated from Fig. 5.2 is 6×10^{-5} ohms/deg which is in agreement with that for bulk molybdenum.

The major problem with this material and the method of preparation is the influence of moisture during the plasma spray process. This is a significant factor when commercial spraying sources are employed. This causes the production of interfacial layers of molybdenum bronzes, H_xMoO_y, which result in loss of adhesion. However, this can be avoided on precursor Na/K ceramics with special care and strongly

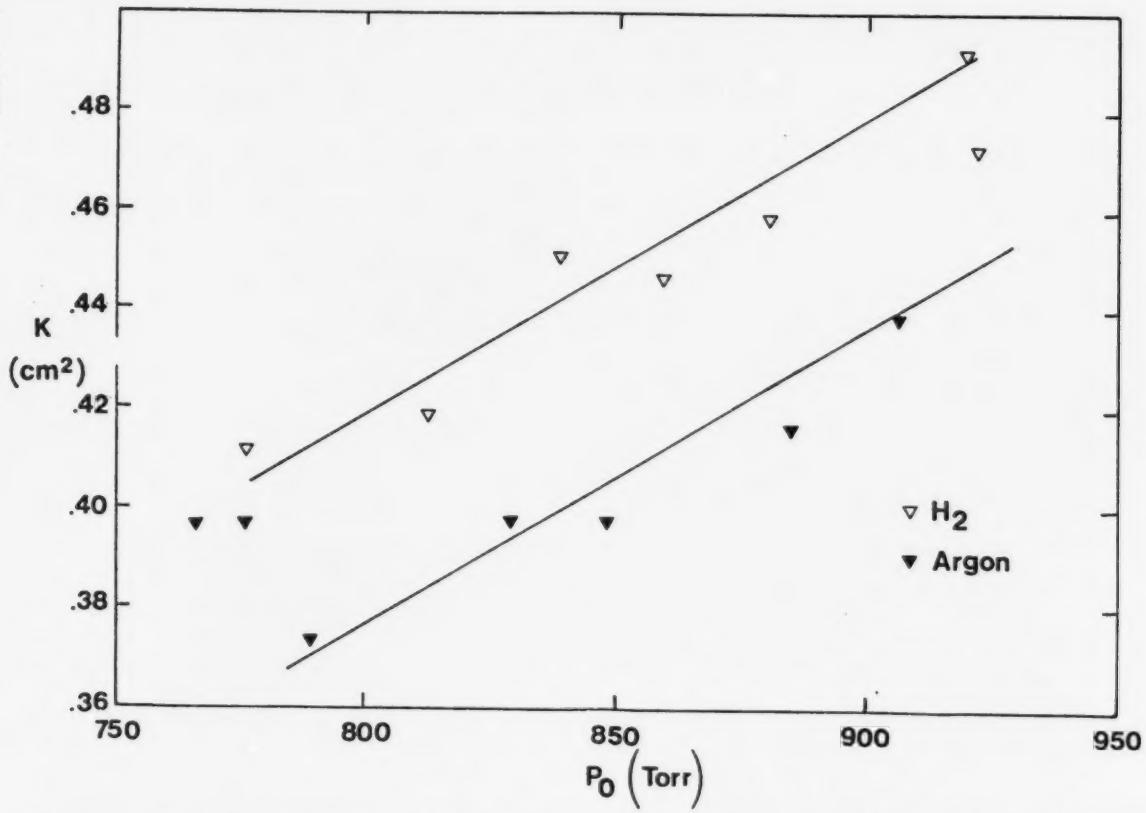

Figure 5.1:Permeability coefficient K versus pressure for Mo.

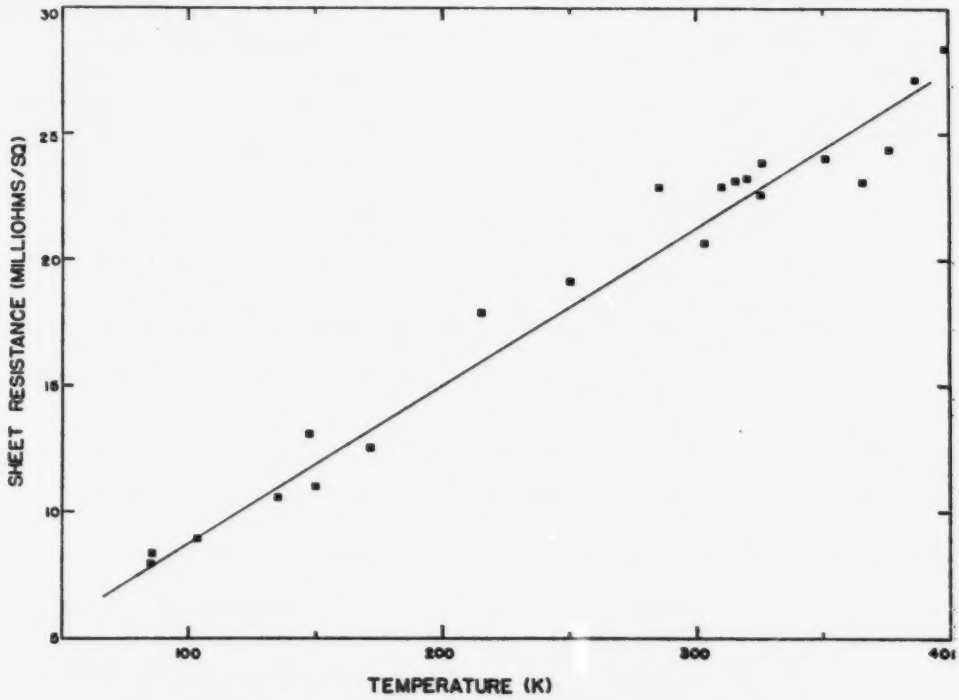

Figure 5.2 $\rho_{\square}$ versus T for plasma sprayed Mo.

adherent films can be produced. The nature of the surface also plays a role. In the case of Na-β-aluminas, poor adhesion has been noted on 'Ceramtec' Li-stabilised aluminas. This is due both to a smooth outer surface and a strong adsorption of water for this stabiliser. These problems are virtually absent for material developed by Almax Industries which has a rougher surface and employs Mg-stabilisation. It is unlikely that Mo will be applicable to fully exchanged H_3O^+ β/β'' aluminas for this reason, but the film does withstand the exchange process.

The above properties indicate that molybdenum is an excellent candidate for the hydrogen electrode, although its catalytic activity have not yet been proved. Future work should also define the optimum preparation conditions to avoid interfacial layer formation.

5.2 Nickel Cobalt Oxide

$NiCo_2O_4$ has been shown to be an excellent oxygen electrode for alkaline water electrolysis where the highest catalytic activity is obtained for the spinel phase of the general formula AB_2O_4 [4,5,11] . However, neither Ni or Co prefer the +3 oxidation state and the question arises as to which ions reside in the A (+2) and B (+3) sites. By indirect experiments [5], it has been proposed that there exists a compromise given by the formula:

$$Co^{2+}_{1-a}\ Co^{3+}_{a}\ [\ Ni^{2+}_{1-b}\ Ni^{3+}_{b}\ Co^{3+}\ ]\ O^{2-}_{3+a+b}\ V_{o\,(1-a-b)/2}$$

where the oxygen vacancy, V_o is included for electro-neutrality. In our experiments which utilise films fabricated from dried gel solutions, no discernable peaks are obtained in the x-ray powder diffraction patterns. This indicates that the films are amorphous, or as is more likely, consist of very small crystallites. This has important consequences in terms of the porosity and resistivity discussed in this section.

Resistivity measurements as a function of temperature show some unusual aspects which are related to oxygen adsorption-desorption processes. The measurements were carried out by the van der Pauw technique and by the measurement of the resistance of a sheet of material between two silver paint contacts. The latter was most convenient for controlled atmosphere experiments. The results are illustrated in Fig.5.3.

In argon, the initial resistance of a freshly made film decreased as the temperature was raised to 100°C (A-B). However, if the temperature was decreased and then cycled, the resistance changed with an activation energy of about 0.15 eV (B-C-D-E). If the temperature was increased to above 200°C, the change in resistance became more pronounced as oxygen was desorbed from the film (F-G). If the atmosphere is now changed to pure oxygen, the process is reversed and the resistance can be reduced almost back to its starting value (G-H-I-J-K-L). It is clear that oxygen plays a major role in the conductivity of this material.

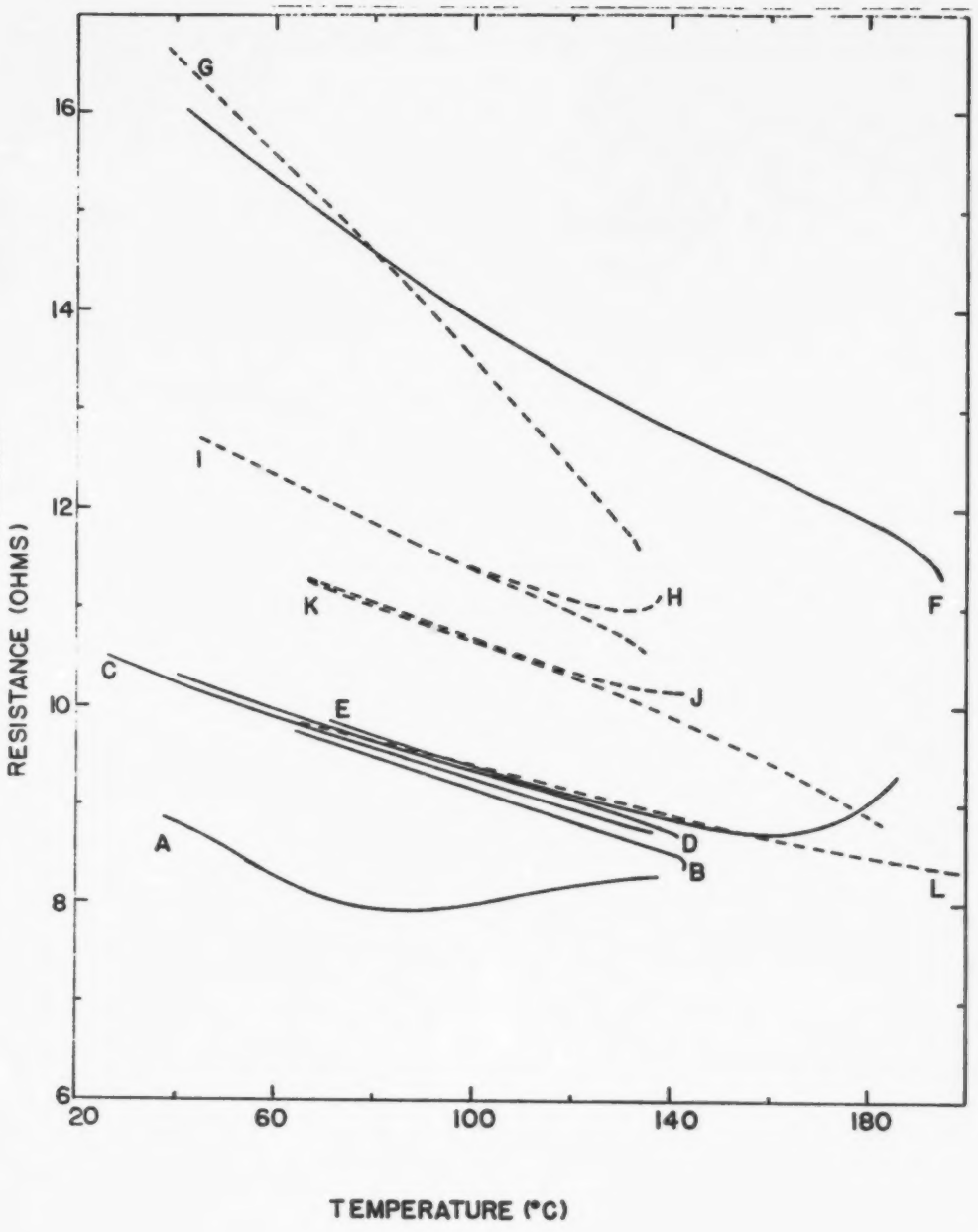

Figure 5.3: Resistance vs temperature for a $NiCo_2O_4$ film on glass. The graph shows the film resistance during several temperature cycles, first in argon and then in oxygen.

This behaviour can be explained in a number of ways:

a) Semiconductivity In such a complex oxide, the band structure is determined not only by the intrinsic crystal properties, but also by carrier migration between multi-valent states of the metal ions. Such materials frequently can be described as semiconductors having a small band gap, or as small polaron conductors having an activated mobility.

b) Oxygen ion (or vacancy) conductivity The incorporation of an oxygen ion vacancy in the chemical formula given above suggests that this may be a possible mechanism. However, from the properties of similar materials, it is unlikely that the ion mobility would result in adequate ionic conductivity at room temperature.

c) Surface conductivity The oxygen content may influence the electronic conductivity in the surface regions by modifying the available valence states and by changing the probability for electronic hopping conduction.

It is difficult to distinguish between these mechanisms and experiments such as Hall Effect have proved inconclusive. The small negative Hall coefficient observed is generally consistent with what is observed for low mobility semiconductors. However, it should be noted that surface conductivity would be enhanced by the small crystallite size and consequent large surface area deduced from the x-ray powder diffraction results. Such a mechanism is most likely electronic in nature. Since the absorption of oxygen is a

pre-requisite for good catalytic action, this material is promising for an electrode material.

The small crystallite size also plays a role in determining the porosity. It was found that low resistance films could only be achieved on glass frits by the successive application of a large number of coats. This is related to the fluidity of the solution and to the subsequent small particle size. Fig. 5.4 shows that this results in low porosity, where measurements indicate an average pore radius of $4.0 \pm 0.5\,\mu m$ making these films the least porous of the materials studied.

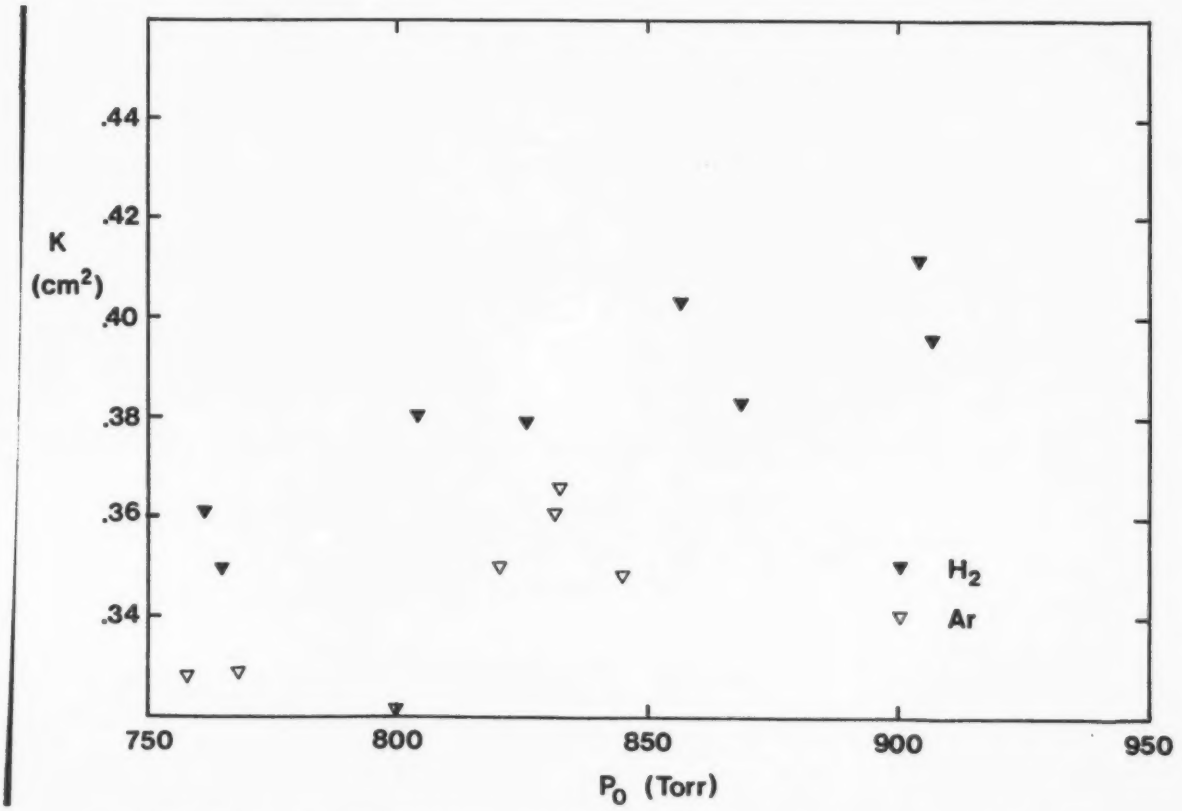

Figure 5.4: Permeability coefficient versus pressure for $NiCo_2O_4$.

5.3 Ruthenium Dioxide

RuO_2 is known to be a good catalyst for the oxygen reaction and can easily be prepared by decomposition of an acqueous solution of ruthenium chloride. X-ray measurements showed that the black film produced was crystalline, but the diffraction pattern could not be indexed making the crystalline structure uncertain. Moreover, in contrast to $NiCo_2O_4$, low resistance films could be achieved with two or three coats (Fig.5.5)

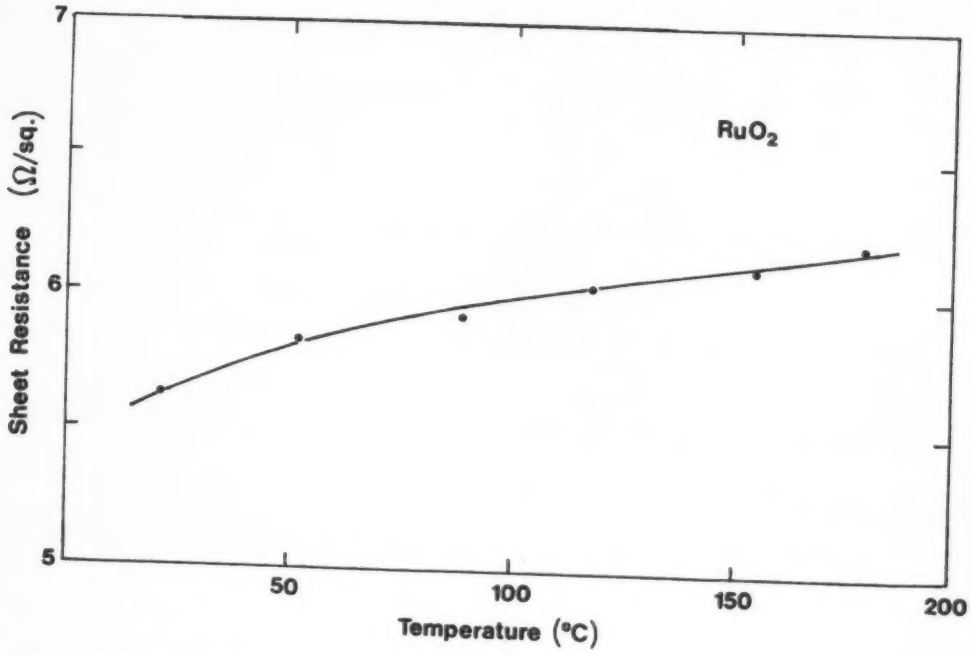

Figure 5.5: $\rho_{\square}$ versus T for RuO_2

The film had good porosity with a mean pore radius of the order of 4.3 ± 0.5 μm.

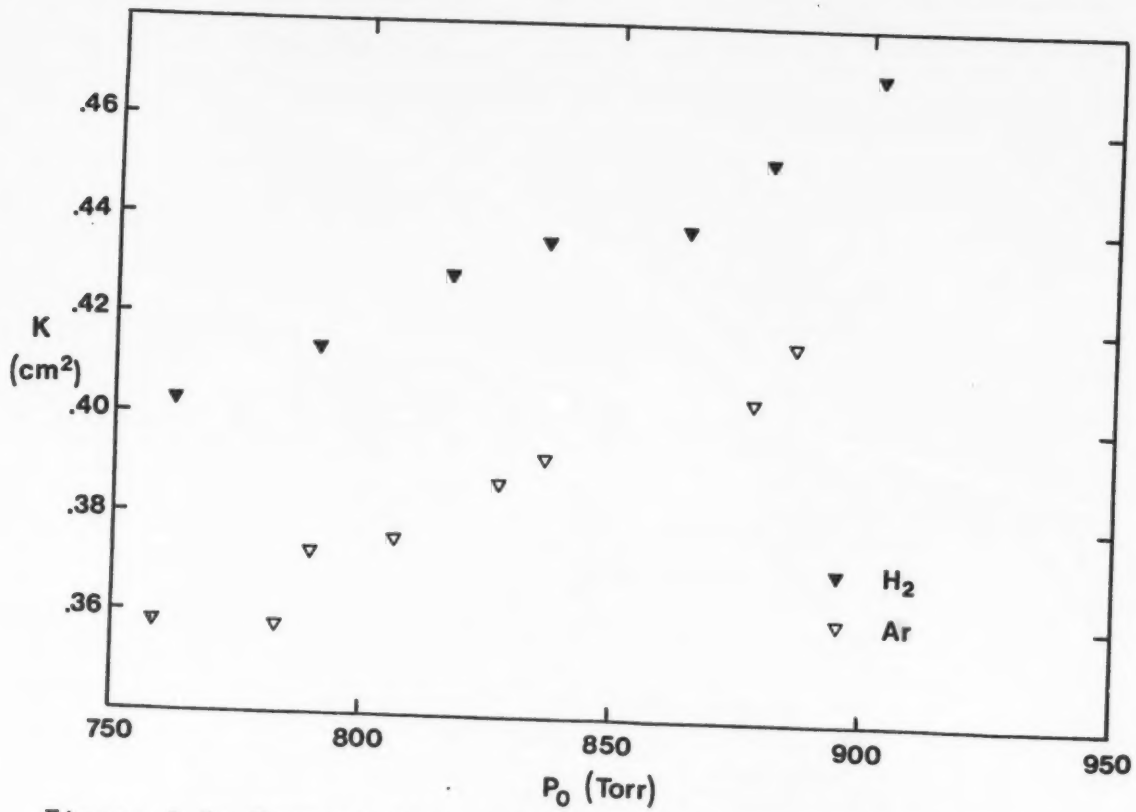

Figure 5.6: Permeability coefficient K versus P for RuO_2.

This material has obvious value as an oxygen electrode material but the starting material is very expensive making it unattractive for a commercially viable fuel cell.

6. Steam Cell Design and Lifetime Measurements

Lifetime performance and material function at temperatures > 150°C were evaluated in two types of cell. The first utilised a glass apparatus - Fig.6.1

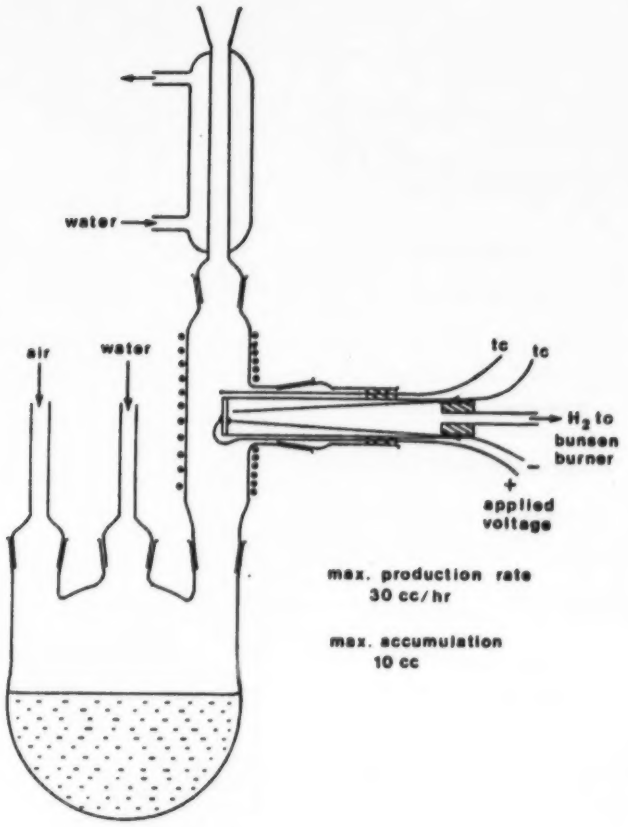

Figure 6.1: Schematic representation of a steam cell

In this case the β-alumina samples were coated with the appropriate electrode and were sealed into an alumina tube using Cerambond high temperature cement and RTV rubber sealing compound. Platinum wire contacts were made to each side. Although this apparatus allowed adequate experimentation at temperatures below 100°C, it was not possible to exceed this even with additional heater coils.

A high temperature design involving a heat exchanger is shown in Fig.6.2. This is constructed of stainless steel and the incoming and outgoing steam paths overlap. This has been operated up to 300°C.

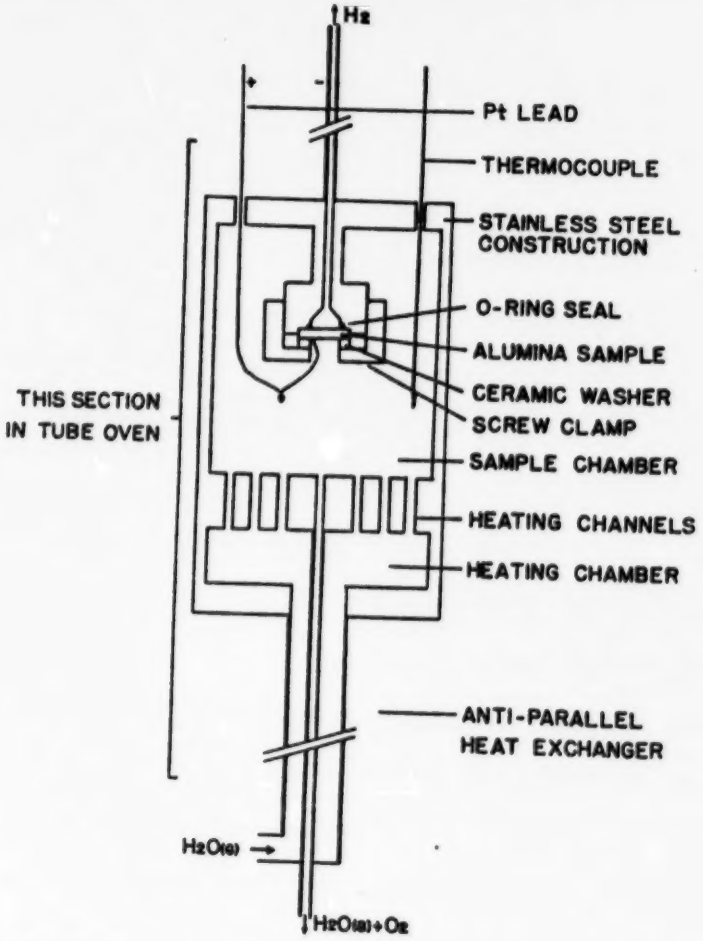

Figure 6.1: High temperature steam cell

In this case the β -alumina samples were coated with the appropriate electrode and were screwed into an stainless steel holder using RTV cement constrained to act as an o-ring seal. Platinum wire contacts were again made to each side. This apparatus allows effective operation as a fuel cell, although seals continue to be a problem for continued operation at 300°C.

6.1 Electrode Lifetime

Measurements on lifetime performance have been limited by the availability of reproducible electrolyte. Lifetime studies have been carried out with platinum electrodes, molybdenum and nickel cobaltate - the latter two in one cell. To the extent of the results to date, all three systems are stable in steam to 300°C.

Platinum

As noted above, a problem has been identified with stability of platinum electrodes on hydronium β"aluminas in acid environments. The best performance is found for films fired in hydrogen and it seems necessary to set limits on the pH of the contact electrolyte. This should be controllable within a steam cell. Non-porous films due to poor preparation or a residue of organics show a tendency to flake at high hydrogen currents. The platinum electrode has non-blocking behaviour when measured using complex impedance methods. The data shown in Fig.6.3 was obtained on an electrolysis cell operating at 100°C [12] and is consistent with a reversible nature for the interface.

Molybdenum/$NiCo_2O_4$

A cell with the above electrodes was established and operated to 300°C in steam with little visible deterioration in electrode appearance. The initial currents were comparable with those in cells having platinum electrodes. Unfortunately, the cell seals degraded before measurements of cell performance could be made.

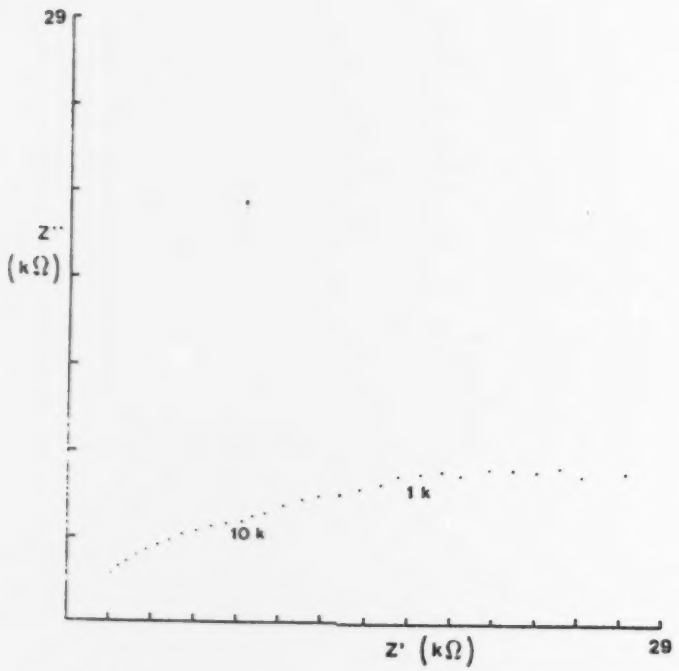

Figure 6.3: Complex impedance diagram for water electrolysis cell using platinum/platinum electrodes.

The difficulty with lifetime measurements at 300°C is less the electrode materials - the two candidates indentified in this contract seem to have reasonable properties, but the corrosion of the cell seals and current collectors. The electrolyte stability also requires further attention, with consideration of the extent to which full exchange is possible or necessary. A consequence of partial exchange is the continuation of the ion exchange process in the steam cell with the resulting migration of alkali ions to the electrode interface. A possible advantage for an electrode system would be the ability to absorb a limited amount of alkali during the initial stages of cell lifetime. Mo does allow the access to Na - hence its use as an electrode in in devices utilising Na-β-alumina. However the properties of spinels such as $NiCo_2O_4$ to allow alkali absorption at the oxgyen electrode is obviously more important given the polarity of the applied cell voltage.

7. SUMMARY AND CONCLUSIONS

In the first year of this contract, six materials were selected as candidate electrodes for hydrogen-air fuel cells and the general electrochemical background for electrolysis and fuel cell operation using solid electrolytes was reviewed [13-14]. In the current year, it was shown that high porosity films of molybdenum could be produced by the commercially- viable plasma spray technique. Moreover, these exhibited excellent electrical properties making molybdenum the prime choice for the hydrogen electrode. In contrast, the choice of oxygen electrode material proved more difficult.

Attempts to prepare lanthanum nickelate by R.F. sputtering resulted in lathanum-rich phases which would be deleterious to cell performance. Although it was felt that this problem could be solved by careful control of the sputtering parameters, film thicknesses and deposition rates are small and are such as to make future commercialisation improbable. Research on this material was therefore discontinued. More success was achieved with nickel cobalt oxide $NiCo_2O_4$ produced by an attractive chemical deposition route. Although the films had the lowest porosity of the materials tested, they showed excellent conductivity and stability in steam. The conductivity showed a strong dependence on the atmosphere, and as this is indicative of catalytic activity the material is a strong contender for future use. The remaining material - ruthenium dioxide, showed some good properties, but its expense makes it a

remote possibility for commercial application.

Thus this work has defined two materials - molybdenum and nickel cobalt oxide as showing promise as electrodes for a hydrogen/air fuel cell. Both form adherent coatings with adequate porosity and are stable in the steam cell enviroment. Although the work on lifetime evaluation was limited by electrolyte and seal problems, the preliminary results are encouraging and future work should address optimisation of the preparation procedures and how these affect the catalytic activity. This is particularly important in the case of $NiCo_2O_4$ which has exhibited some particularly interesting properties.

Acknowledgments

Thanks are due to L.Devlin, B.Judd, J.Wiseman and Y.Koskinen for contributions to this work. The assistance of Mrs Edith Swan on the administrative side is appreciated.

REFERENCES

1. M.F.Bell, M.Sayer, P.S.Nicholson and M.Z.A.Munshi
Development of Electrodes for Solid Electrolytes
DSS Contract # OST83-00139

2. M.Sayer, M.F.Bell, P.S.Nicholson and K.Yamashita
The Selection,Preparation and Characterisation
of Ceramic Hydrogen Ion Conductors - Phase IV
DSS Contract # OSX82-00120

3. D.S.Smith - M.Sc Thesis, Queen's University, 1982

4. W.J.King and A.C.C.Tseung,
Electrochimica Acta 19,(1974),493

5. W.J.King and A.C.C.Tseung,
Electrochimica Acta 19,(1974)

6. S.B.Krupanidhi and M.Sayer, J.Appl.Phys. 56,(1984),3308

7. L.J.van der Pauw, Phil.Res.Reps. 13,(1958),1

8. K.A.S.Malinaus and E.A.Mason Gas Transport in Porous Media:The Dusty Gas Model Elsevier (Amsterdam 1983)

9. E.A.Mason and R.B.Evans III, J.Chem.Educ.,46,(1969),358

10. R.B.Evans,III, L.D.Love, and E.A.Mason,
J.Chem.Educ.,46,(1969),423

11. G.Feuillade,R.Coffre, G.Outhier,
Ann.de Radioelect. 21,(1966), 105